Microspheres of New Alternating Copolyesters Derived from Glycolic Acid Units for Controlled Drug Release

Meritxell Martínez-Palau, Lourdes Franco, Jordi Puiggalí

Departament d'Enginyeria Química, Escola Tècnica Superior (ETS) d'Enginyeria Industrial, Universitat Politècnica de Catalunya, Diagonal 647, Barcelona E-08028, Spain

Received 14 February 2008; accepted 23 May 2008
DOI 10.1002/app.28777
Published online 7 August 2008 in Wiley InterScience (www.interscience.wiley.com).

ABSTRACT: Two new copolyesters consisting of an alternating disposition of glycolic acid units and 4-hydroxybutyric or 6-hydroxyhexanoic units were assayed in the form of microspheres as drug delivery systems. Despite their similar chemical constitutions, great differences in properties such as the melting point and glass-transition temperature were found between the two polymers. Microspheres could be successfully prepared by the oil/water emulsification/solvent evaporation method and revealed different morphological features depending on the polymer matrix. The encapsulation and release of triclosan in a cell medium and in a Sörensen solution were evaluated. The release profiles, which were clearly different in both polymers when the hydrophobic cell medium was employed, indicated that the release reached an asymptotic value that was always lower than the maximum release expected for the drug loading. No significant degradation occurred during drug release. The charged microspheres of both polymers were highly crystalline, and the incorporation of drug particles into the polymer crystalline domains was feasible. No trace of single triclosan crystals was found in differential scanning calorimetry or X-ray synchrotron experiments. © 2008 Wiley Periodicals, Inc. J Appl Polym Sci 110: 2127–2138, 2008

Key words: biological applications of polymers; drug delivery systems; polyesters

INTRODUCTION

Controlled drug release employs drug-encapsulating devices from which therapeutic agents can be released at controlled rates for long periods of time ranging from days to months. Such systems offer numerous advantages over traditional methods of drug delivery, including the tailoring of drug release rates, protection of fragile drugs, and increased patient comfort and compliance.

Polymeric microspheres are ideal vehicles for many controlled delivery applications because of their ability to encapsulate a variety of drugs and their sustained drug release characteristics.[1–3] Aliphatic polyesters constitute the most important group of materials for such applications because they may meet some prerequisites, such as biocompatibility, processability, and resorption of degradation products.[4,5] Within this family, polymers derived from glycolic acid, lactic acid, and 6-hydroxyhexanoic acid or their copolymers are nowadays receiving increasing interest.[6–8] However, there are problems concerning the bulk-degradation mechanism of polymer matrices, such as those observed for polyglycolide and polylactide devices.[9,10]

Different techniques have been developed to prepare polymer microspheres useful for drug release,[11] among which organic solvent evaporation and extraction methods are the most common.

It is well known that the degradation rate and, in general, material properties can be controlled through copolymerization, which allows both the composition and chemical microstructure to be modified. We have recently developed a synthesis procedure to obtain polyesters[12,13] consisting of glycolic acid and ω-hydroxyl acid units with a regular sequence distribution and high yields (Scheme 1). This new synthesis is based on a thermal polycondensation reaction in which the formation of a metal halide salt becomes the driving force of the process.[14–17] The great simplicity of this method and the possibility of changing final properties by the use of a different ω-hydroxyl acid comonomer have raised interest in this family of polymers, which are characterized by a semicrystalline character. This feature contrasts with the more amorphous nature of copolymers prepared by ring-opening polymerization,[18–20] which usually renders an irregular sequence distribution. Cytotoxicity studies have

Correspondence to: J. Puiggalí (jordi.puiggali@upc.es).
Contract grant sponsor: Centro de Investigación Científica y Tecnológica.
Contract grant sponsor: Fundo Europeu de Desenvolvimento Regional; contract grant number: MAT 2006-02406.

© 2008 Wiley Periodicals, Inc.

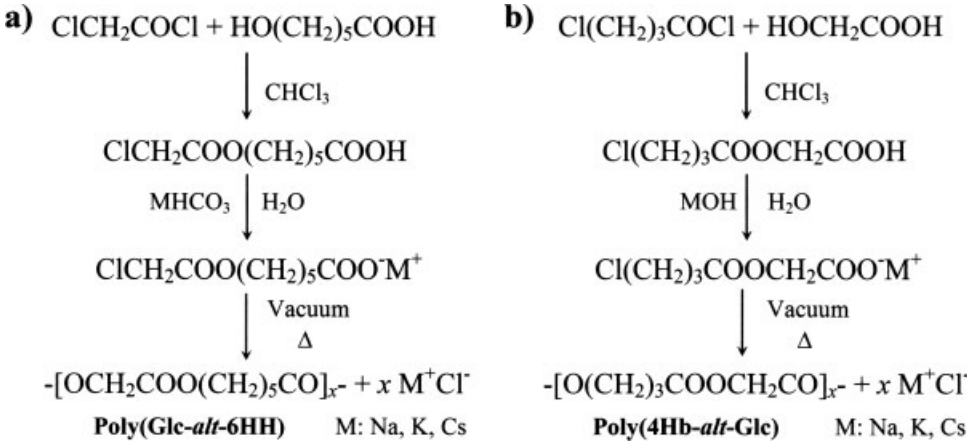

Scheme 1.

recently been undertaken with promising results for future biological applications for the studied copolymers.[21]

The aim of this work was the study of the characteristics of microspheres prepared from two representative copolyesters with very different properties. These samples corresponded to the 4-hydroxybutyric and 6-hydroxyhexanoic copolymers of glycolic acid, which hereafter are named poly(4Hb-*alt*-Glc) and poly(Glc-*alt*-6HH), respectively. Furthermore, the release of drugs such as triclosan (2,4,4′-trichloro-2′-hydroxydiphenyl ether; Scheme 2) was also evaluated. This drug can serve as a model of a hydrophobic material with the added advantage of easy detectability. Triclosan has a well-demonstrated antimicrobial effect[22] and has received much attention as far as topical applications are concerned, including some specialized ones such its incorporation into commercial sutures.[23,24] Furthermore, the controlled release of triclosan from microspheres has also recently been investigated for application to the oral cavity[25,26] and as a malaria treatment.[27]

EXPERIMENTAL

Polymer synthesis

Poly(Glc-*alt*-6HH) was synthesized by the thermal polyesterification of the potassium salt of 6-(2-chloroacetate)hexanoic acid, as previously reported,[13] with an 80% yield [Scheme 1(a)]. Poly(4Hb-*alt*-Glc) was synthesized by the thermal polyesterification of the potassium salt of 4-chlorobutyric acid carboxymethyl ester, as previously reported,[12] with an 80% yield [Scheme 1(b)].

Molecular weight determination

The molecular weight distribution and polydispersity index were measured by gel permeation chromatography with a Shimadzu (Kyoto, Japan) model LC-8A system equipped with the Empower computer program (Waters, New Castle, DE). Average molecular weights were calculated with poly(methyl methacrylate) standards. A PL HFIPgel 300 × 7.5 mm column (Polymer Lab, Darmstadt, Germany) and a refractive-index detector (RID-10A, Shimadzu) were used. Polymers were dissolved and eluted in hexafluoroisopropanol containing CF_3COONa (0.05*M*) at a flow rate of 0.5 mL/min (injected volume = 10 μL, sample concentration = 1.5 mg/mL).

Preparation of the microspheres

Microspheres were prepared by the oil/water emulsification/solvent evaporation method. Typically, 2 g of the polymer and 0.3 g of triclosan were dissolved in 40 mL of dichloromethane. The resulting solution was poured into 500 mL of an aqueous solution of 0.8% (w/v) poly(vinyl alcohol) (87–89% hydrolyzed; weight-average molecular weight = 13,000–23,000) and 1% (w/v) sodium chloride under vigorous stirring with a paddle at 1,300 rpm. The oil/water emulsion was kept under stirring until the evaporation of dichloromethane was observed. Microspheres were collected by filtration, washed with distilled water, and allowed to dry overnight in a watch glass

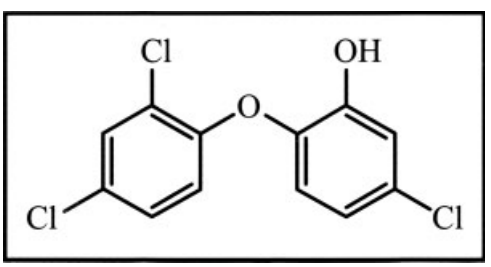

Scheme 2.

dish and then were stored in a desiccator *in vacuo* (0.1 mmHg) before use to make sure that the dichloromethane was removed.

Particle size analysis: granulometry

Microspheres were separated into micrometric fractions by the application of vibrations to sieves with average pore sizes of 1000, 500, 250, 125, 100, 80, and 45 μm. The resulting fractions were weighed to determine the size distribution. Values were obtained in triplicate.

Scanning electron microscopy

For scanning electron microscopy, microspheres were fixed on supports with a double-coated carbon adhesive sheet and covered with gold with a sputter coater (Balzers SCD 004, Balzers, Liechteinstein). Samples were then observed on a JEOL (Tokyo, Japan) JSM 6400 scanning microscope at 20 kV.

Differential scanning calorimetry (DSC)

Thermal analysis was performed by DSC with a Thermal Analysis Q100 instrument (New Castle, DE) with T_{zero} technology to determine the temperature and heat of fusion of the microsphere samples. Indium metal was employed for the temperature and enthalpy calibration. All experiments were performed under an N_2 flow at a heating rate of 20°C/min.

Physical state of the polymer and triclosan in the microspheres

Wide-angle X-ray diffraction (WAXD) and small-angle X-ray scattering (SAXS) experiments were conducted to investigate the crystalline structure of the microparticles and the physical state of the drug in the microspheres with the synchrotron X-ray radiation source (wavelength = 0.9797 Å) at the CRG beam line (BM16) of the European Synchrotron Radiation Facility (Grenoble, France). The detectors were calibrated with the different diffractions of standards of an alumina (Al_2O_3) sample and silver behenate for WAXD and SAXS, respectively. The diffraction profiles were normalized to the beam intensity and corrected with consideration of the empty sample background. Deconvolution of WAXD peaks was performed with the PeakFit v4 program from Jandel Scientific Software with a mathematical function known as the Gaussian and Lorentzian area. The calculation of the correlation function and the corresponding parameters was performed with the CORFUNC program,[28] which was provided by Collaborative Computational Project 13 for Fibre Diffraction/Non-Crystalline Diffraction.

Determination of the drug loading

The drug loading was determined on a double-beam ultraviolet–visible spectrophotometer (Cary 100 Bio, Varian, Victoria, Australia). About 10 mg of triclosan-containing microspheres was accurately weighed and dissolved in $CHCl_3$, and the solution was then brought to a 25-mL volume. The absorbance was measured at 281 nm, and triclosan was quantified by the interpolation of the absorbance values of the samples with the linear equation ($r^2 > 0.999$) obtained from standard solutions. Absorbances were corrected with measurements of the blank samples corresponding to solutions with the same polymer concentration, which had a very small (0.1%) influence in the baseline of the ultraviolet spectrum. Each experiment was conducted in triplicate, but only average values were reported.

In vitro drug release

In vitro drug release was investigated at 37°C in an incubator shaker operated at a stirring speed of 60 rpm. Each experiment was conducted in triplicate or sextuplicate (the plotted data resulted from the averages of the corresponding determinations at each time point). About 10 mg of drug-loaded microspheres 45–80 μm in diameter was accurately weighed and added to vials filled with 20 mL of Sörensen solution or cell media [consisting of Dulbecco's modified Eagle's medium with 7.5% (w/v) sodium hydrogen carbonate and 10% (v/v) fetal bovine serum adjusted at 7.42].

For the quantitative analysis of triclosan, 100-μL aliquots were taken at appropriate time intervals, filtered with a syringe containing cotton at the needle end, and analyzed by high-performance liquid chromatography (LC-6A, Shimadzu); 20 μL was injected into an Extrasil ODS1 tracer; 3 μm, 10 cm × 0.4 cm column. The eluent was acetonitrile/water/acetic acid (59/39/2 v/v), and the flow rate was 0.8 mL/min. Triclosan was detected and measured by ultraviolet absorbance at 281 nm.

Degradation studies

Hydrolytic degradation assays were carried out at 37°C in a pH 7.42 Sörensen solution (0.1*M* aqueous Na_2HPO_4/KH_2PO_4) containing sodium azide (0.03% w/v) to prevent microbial growth. Samples were prepared in glass vials. Typically, 10 mg of drug-free polymer microspheres (diameter = 45–80 μm) was added to 20 mL of the aforementioned solution. The remaining particles were collected by filtration at predetermined time intervals. Experiments were performed in triplicate.

TABLE I
Molecular Weight Data for the Synthesized Polyesters

Polymer	M_n (g/mol)	M_w (g/mol)	D	Intrinsic viscosity (dL/g)[a]
Poly(4Hb-*alt*-Glc)	8,000	20,000	2.5	0.47
Poly(Glc-*alt*-6HH)	11,000	35,000	3.1	0.73

D = polydispersity index; M_n = number-average molecular weight; M_w = weight-average molecular weight.
[a] Measured in dichloroacetic acid at 25°C.

TABLE II
Yield, Drug Content, and Encapsulation Efficiency of the Microspheres

Microsphere type	Yield (%)[a]	Drug loading (% w/w)[b]	Encapsulation efficiency (%)[c]
Poly(4Hb-*alt*-Glc)	53 ± 2.5	11.3 ± 1.2	46.2 ± 2.1
Poly(Glc-*alt*-6HH)	72 ± 4.3	11.6 ± 1.6	63.6 ± 4.2

[a] Yield = Weight of the microparticles/(Weight of the drug + Weight of the polymer). The data correspond to the media of three different batches.
[b] Drug loading = Weight of the drug within the microspheres/Weight of the microspheres. The data correspond to the media of three determinations of microspheres 45–80 μm in diameter.
[c] Encapsulation efficiency = Weight of the drug within the microspheres/Weight of the drug added during the microsphere synthesis. The data correspond to the media of three determinations.

RESULTS AND DISCUSSION

Polymer synthesis

Poly(Glc-*alt*-6HH) and poly(4Hb-*alt*-Glc) samples were prepared as described previously. The molecular weights and viscosimetry data are summarized in Table I.

Encapsulation efficiency and morphology of the microparticles

The drug loadings and efficiencies of entrapped triclosan are summarized in Table II. The drug loadings for the 45–80-μm-diameter sieve fraction were similar and close to 11.5% for both kinds of microspheres. However, large differences were found between the two copolyesters in terms of the yield

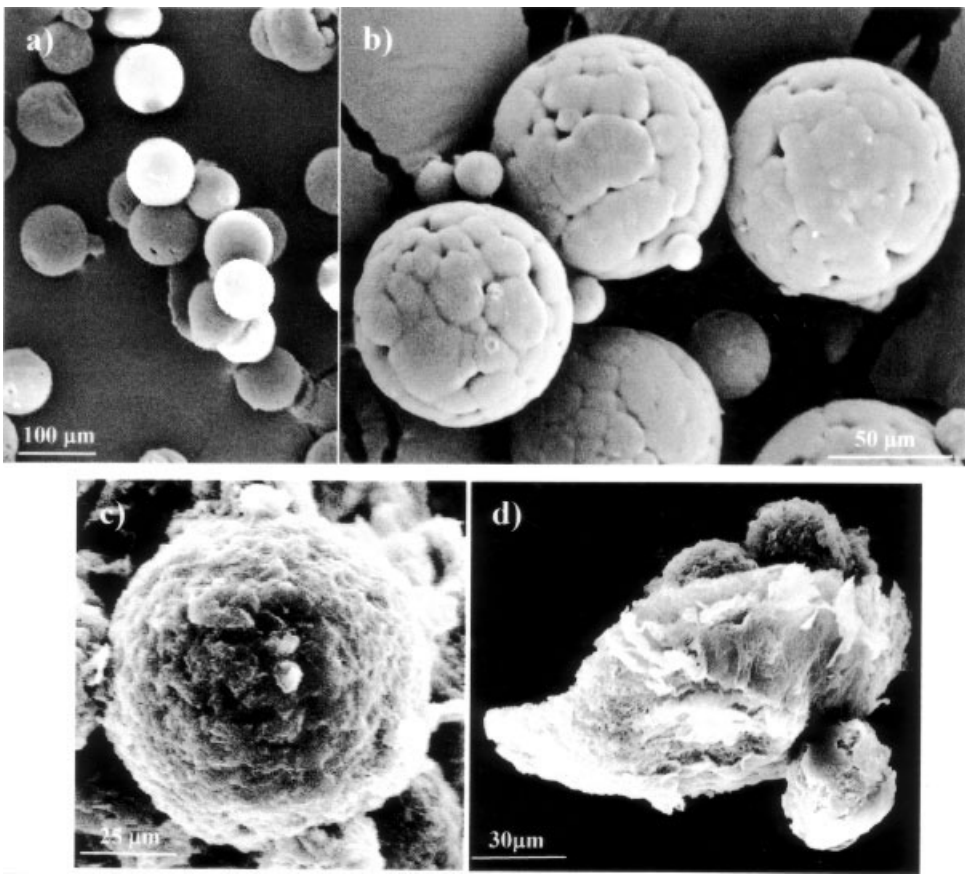

Figure 1 Scanning electron micrographs of triclosan-charged microparticles of (a,b) poly(Glc-*alt*-6HH) and (c,d) poly(4Hb-*alt*-Glc). In all cases, sieve fractions were between 45 and 80 μm. (a) A homogeneous size distribution was observed at a low magnification. (b,c) Clear differences in the surfaces of the two polymers could be observed at a high magnification. (d) A degraded sample of uncharged poly(4Hb-*alt*-Glc) microparticles is shown.

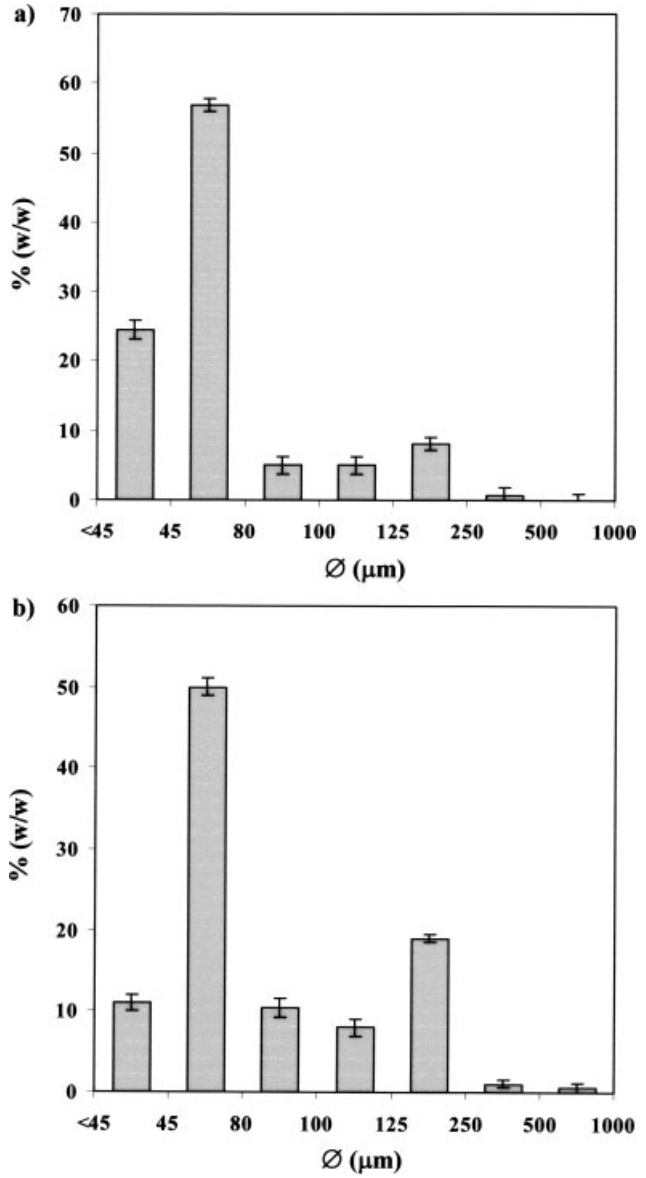

Figure 2 Bimodal size distributions of (a) poly(Glc-*alt*-6HH) and (b) poly(4Hb-*alt*-Glc) microspheres prepared by the oil/water emulsification/solvent evaporation method (ϕ = diameter).

and encapsulation efficiency. The highest values were obtained with the most hydrophobic polymer [poly(Glc-*alt*-6HH)], which could establish better intermolecular interactions with triclosan. For this reason, the encapsulation efficiency increased from 46 ± 2 to 64 ± 4%; this is a significant difference if we consider the Student *t* test (95% confidence level). Other factors, such as the affinity of the drug for aqueous and organic phases, emulsion stability, and microparticle size, may also be considered,[29] but in this case, they did not seem to play a significant role.

The microparticles of both polyesters were essentially spherical (Fig. 1) and had a bimodal size distribution (Fig. 2). The 45–80-μm-diameter sieve fraction was always the predominant one under the given preparation conditions and was used for the release experiments. The microsphere surfaces were clearly different, depending on the polymer matrix. Thus, a rough surface and high porosity were characteristic of the poly(4Hb-*alt*-Glc) microparticles [Fig. 1(c)], whereas a smooth surface composed of small domains having a globular geometry was observed in the poly(Glc-*alt*-6HH) microparticles [Fig. 1(b)]. It has been reported that the morphology is determined during microsphere hardening as the organic solvent evaporates during preparation.[30] In our case, a smoother surface was observed for the most hydrophobic polymer matrix, which, in addition, corresponded to the stickiest sample, as deduced from the thermal properties. After exposure to the degradation medium, a change in the geometry could be detected for the larger and initially more irregular microspheres [Fig. 1(d)].

Crystallinity of the copolyester microspheres: the physical state of triclosan in the microspheres

DSC heating scans corresponding to both uncharged and triclosan-loaded poly(4Hb-*alt*-Glc) samples that were previously quenched from the melt state are shown in Figure 3. A glass-transition temperature close to −16°C was observed in both cases, and consequently, chain mobility in the amorphous polymer phase did not seem to be highly influenced by the

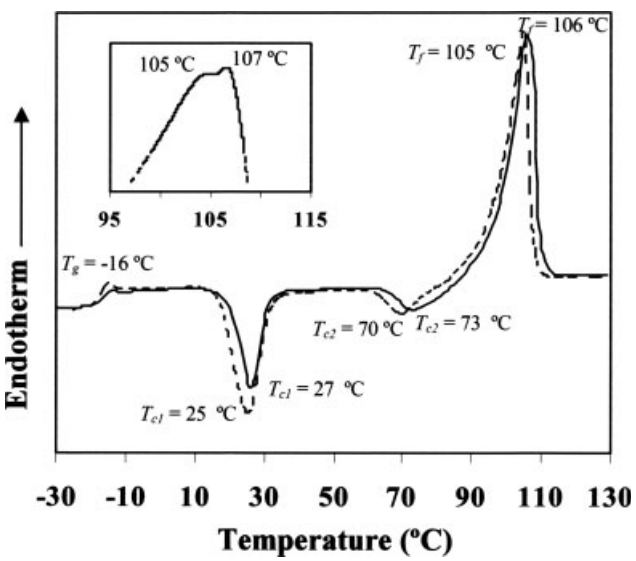

Figure 3 DSC heating scans of (—) uncharged and (- - -) triclosan-charged microparticles of poly(4Hb-*alt*-Glc). Samples were previously quenched from the melt. The inset shows a magnification of the melting peaks observed during the first heating scan of the charged microspheres (T_{c1} = first crystallization temperature; T_{c2} = second crystallization temperature; T_f = melting temperature; T_g = glass-transition temperature).

incorporation of 11.3% triclosan. However, the increase in the calorific capacity was slightly higher for the charged sample, which in addition showed a clear hysteresis peak suggesting a higher amorphous content. Cold and hot crystallization peaks could also be clearly observed in both samples. The crystallization peaks of the triclosan-loaded sample always appeared at a lower temperature (i.e., 25 versus 27°C for cold crystallization and 70 versus 73°C for high-temperature lamellar reorganization), and this feature can be attributed to a slight nucleation effect of triclosan. The enthalpies of hot crystallization peaks were similar for the two samples, whereas the charged polymer had a higher cold crystallization enthalpy. The melting enthalpies of the two samples were quite similar (8.6 and 8.7 kJ/mol for the uncharged and charged samples, respectively) and allowed an estimation of the crystallinity close to 33% by consideration of the group contribution theory.[31] The indicated melting enthalpy was higher than the value corresponding to the addition of the cold and hot crystallization enthalpies. This means that a small proportion of the polymer crystallized during quenching. This quantity was larger for the uncharged sample (crystallinity of 17% vs 13%), and this indicated that triclosan hindered the crystallization of the sample during the fast cooling scan. A slightly lower melting temperature was observed for the charged sample, and this suggested that some triclosan molecules were incorporated into the crystalline phase.

The heating scan of the original charged microspheres (Fig. 3, inset) revealed a double melting peak only (105 and 107°C), and this may suggest the coexistence of crystalline phases with different lamellar thicknesses or indeed the incorporation of different triclosan percentages in these phases. In fact, the sample was highly crystalline (53% as deduced from a global melting enthalpy of 13.9 kJ/mol).

Figure 4 shows the thermal behavior of the uncharged and triclosan-charged poly(Glc-*alt*-6HH) samples. The increase in the hydroxyl acid unit length reduced considerably the melting point of the polymer (106 and 64°C for the hydroxybutyric and hydroxyhexanoic derivatives, respectively) and also the glass-transition temperature. The incorporation of triclosan into the polymer had an effect similar to that explained for poly(4Hb-*alt*-Glc) samples, although the changes appeared to be more significant. Thus, a high increase in the calorific capacity at the glass transition could be observed, indicating that the material did not crystallize readily during fast cooling. A cold crystallization peak was observed at 10°C, whereas no peak appeared in the pure polymer sample because, in this case, the polymer crystallized easily during quenching. In both

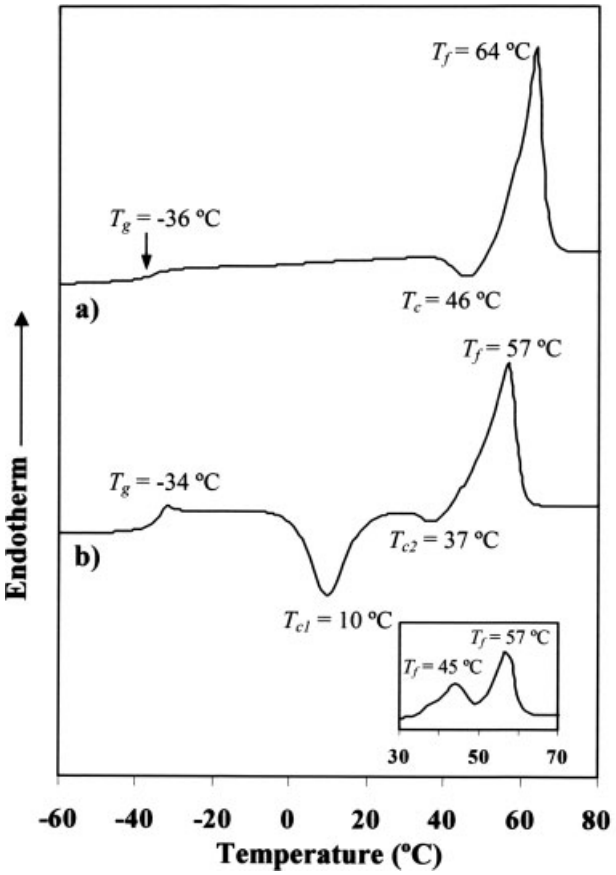

Figure 4 DSC heating scans of (a) uncharged and (b) triclosan-charged microparticles of poly(Glc-*alt*-6HH). The samples were previously quenched from the melt. The inset shows a magnification of the melting peaks observed during the first heating scan of the charged microspheres (T_{c1} = first crystallization temperature; T_{c2} = second crystallization temperature; T_f = melting temperature; T_g = glass-transition temperature).

cases, a small exothermic peak indicative of a lamellar reorganization was seen (46 and 37°C) to some degree before fusion. This fusion was detected as a single endothermic peak that shifted to lower temperatures with the addition of triclosan. This shift (7°C in a sample with an 11.6% concentration of the charged drug) clearly demonstrates that triclosan can be incorporated into the polymer crystalline phase. The thermogram cannot rule out the presence of triclosan crystals because they melt at 55–57°C, that is, in the same temperature range in which the polymer melting peak is detected. In Figure 3, this is not true for the poly(4Hb-*alt*-Glc) samples, and so in this last case, the presence of triclosan crystals can be ruled out according to the DSC scan.

The melting enthalpies of poly(Glc-*alt*-6HH) samples were slightly different (7.3 and 6.3 kJ/mol for the uncharged and charged samples, respectively) and allowed the estimation of crystallinities close to 21 and 19% by the application of the group contribution theory.[31] These values are only approximate

TABLE III
Main Calorimetric Data for Charged and Uncharged Polyesters

Sample	T_{c1} (°C)	ΔH_{c1} (kJ/mol)	T_{c2} (°C)	ΔH_{c2} (kJ/mol)	T_f (°C)	ΔH_f (kJ/mol)
Poly(4Hb-*alt*-Glc)[a]	27	2.9	73	1.2	106	8.6
Poly(4Hb-*alt*-Glc)[b]	25	4.5	70	0.81	105	8.7
Poly(4Hb-*alt*-Glc)[c]	—	—	—	—	105, 107	13.85
Poly(Glc-*alt*-6HH)[a]	—	—	46	0.7	64	7.3
Poly(Glc-*alt*-6HH)[b]	10	4.9	37	0.4	57	6.3
Poly(Glc-*alt*-6HH)[c]	—	—	—	—	45, 57	4.9, 8.5

ΔH_{c1} = first crystallization enthalpy; ΔH_{c2} = second crystallization enthalpy; ΔH_f = melting enthalpy; T_{c1} = first crystallization temperature; T_{c2} = second crystallization temperature; T_f = melting temperature.
[a] Sample after being quenched.
[b] Triclosan-charged sample after being quenched.
[c] Charged microsphere preparation.

and are useful for comparison. More reliable measurements can be obtained from X-ray diffraction, as described later.

The heating scan of the original charged microspheres revealed only a double melting peak (57 and 45°C), which suggested again the coexistence of different populations of crystals. The sample was crystalline (37% as deduced from a global melting enthalpy of 13.4 kJ/mol).

The main calorimetric data of the two studied copolyesters in both charged and uncharged forms are summarized in Table III.

The dispersion of triclosan microparticles in the polymer matrices can also be confirmed by WAXD data, as shown in Figures 5 and 6. The diffraction

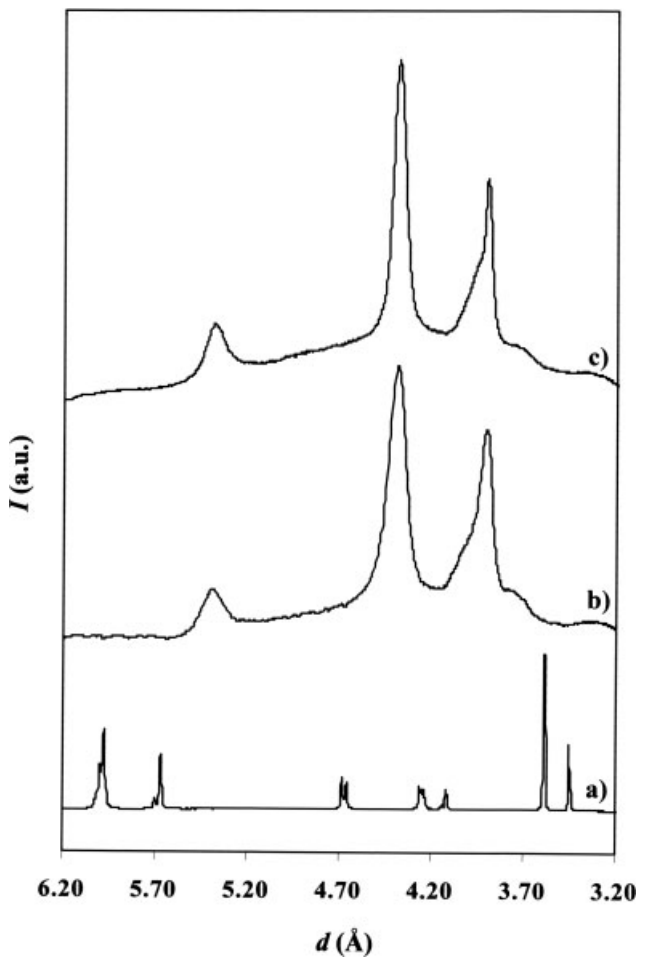

Figure 5 X-ray diffraction patterns of (a) triclosan, (b) poly(4Hb-*alt*-Glc), and (c) poly(4Hb-*alt*-Glc) microparticles containing triclosan.

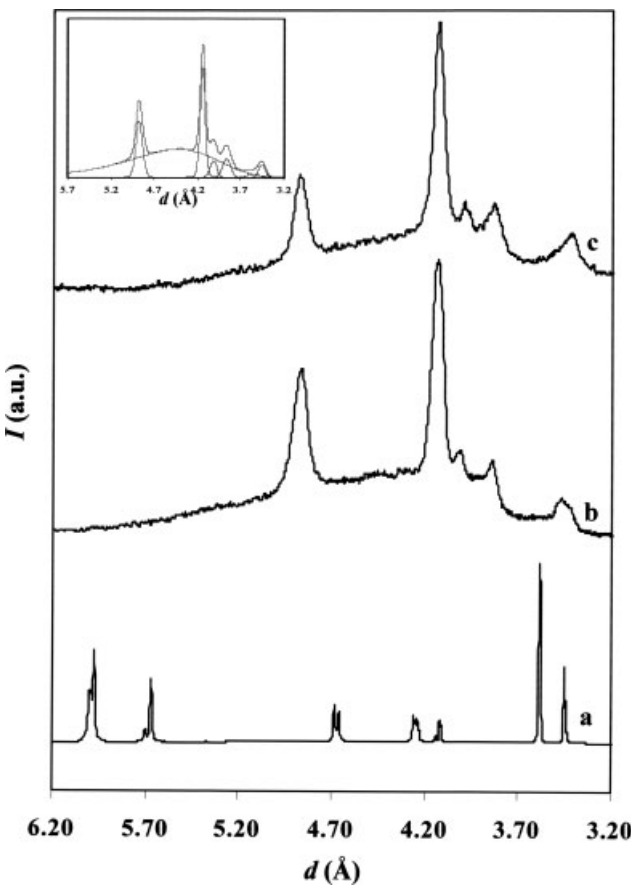

Figure 6 X-ray diffraction patterns of (a) triclosan, (b) poly(Glc-*alt*-6HH), and (c) poly(Glc-*alt*-6HH) microparticles containing triclosan. The inset shows the deconvolution of the WAXD profile corresponding to the charged microspheres.

patterns of microparticles containing triclosan were practically identical to those of the uncharged samples. Note also that triclosan rendered a well-defined diffraction pattern with intense peaks that could not be detected in the charged microspheres, despite their significant drug content ($\sim$ 11.5%).

The crystallinities of charged and uncharged microspheres can be well evaluated by the deconvolution of WAXD patterns and the measurement of the intensities associated with the Bragg peaks (I_B) and amorphous halo (I_{am}; e.g., Fig. 6). The crystallinity deduced from WAXD data (X_c^{WAXD}) is then calculated with the ratio of I_B to ($I_B + I_{am}$). These values seem more realistic than those determined by DSC because they are not based on an estimated value for a 100% crystalline material. Crystallinities of 41 and 53% were determined for the charged and uncharged poly(4Hb-*alt*-Glc) samples, respectively, whereas similar values of 45 and 48% were found for the charged and uncharged poly(Glc-*alt*-6HH) samples, respectively.

Small-angle diffraction patterns are useful for obtaining additional information concerning the lamellar structures of different microparticles and the organization between crystalline and amorphous domains. SAXS profiles [Fig. 7(a)] showed broader peaks at Bragg spacings of 8.8 and 11.5 nm for the charged poly(4Hb-*alt*-Glc) and poly(Glc-*alt*-6HH) microspheres, respectively. The values of this long period remained practically constant independently of the drug load. Figure 7(b) shows the one-dimensional correlation functions calculated for the SAXS profiles. An analysis of the correlation function allows the determination of (1) the long period (L_γ), (2) the crystallinity within the lamellar stacks [the crystallinity deduced from SAXS data (X_c^{SAXS})] and (3) the crystalline lamellar thickness (l_c) and amorphous layer thickness (l_a). Thus, L_γ corresponds to the r value of the first maximum of the correlation function, l_a is assigned to the r value for the intersection of the linear regression in the autocorrelation triangle with the ordinate equal to the first minimum of the correlation function, l_c corresponds to $L_\gamma - l_a$, and X_c^{SAXS} is calculated as l_c/L_γ. The smaller thickness of the two-phase lamellar model was assigned to l_a to obtain an X_c^{SAXS} value higher than X_c^{WAXD}. Table IV summarizes the main morphological parameters deduced for the studied samples.

As usual, the Bragg long period was larger than the L_γ value associated with the most probable distance between the centers of gravity of two adjacent crystals. Thus, the L_γ values were 8.7 and 10.1 nm for the charged microspheres of the hydroxybutyric and hydroxyhexanoic derivatives, respectively. The results deduced from the correlation analysis indicate l_c values close to 5.8 and 7.4 nm for charged poly(4Hb-*alt*-Glc) and poly(Glc-*alt*-6HH) microspheres, respectively. The X_c^{SAXS} values were 67 and 73% for the charged poly(4Hb-*alt*-Glc) and poly(Glc-*alt*-6HH) microspheres, respectively. The ratio of X_c^{WAXD} to X_c^{SAXS} gives an estimation of the volume-filling fraction of the lamellar stacks. This value lies close to 0.6 and points to the existence of amorphous phase domains between the lamellar stacks.

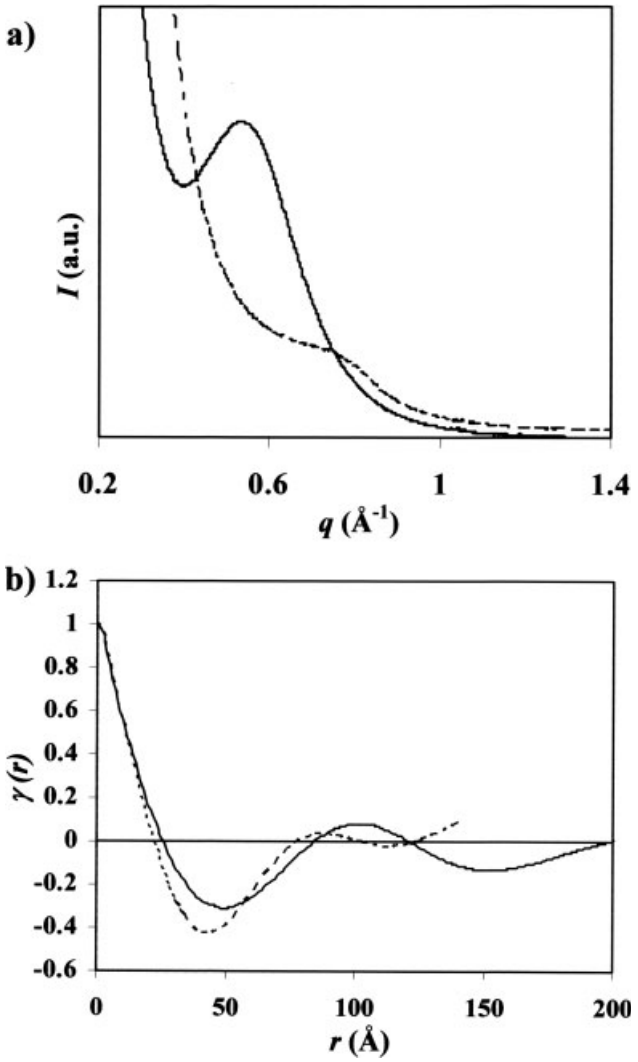

Figure 7 (a) SAXS spectra obtained from charged (- - -) poly(4Hb-*alt*-Glc) and (—) poly(Glc-*alt*-6HH) microparticles (**q** is the scattering vector defined by $4\pi \sin \theta/\lambda$). (b) Normalized one-dimensional correlation function [$\gamma(r)$] of charged (- - -) poly(4Hb-*alt*-Glc) and (—) poly(Glc-*alt*-6HH) microparticles (r is the distance perpendicular to the lamellar stacks).

In vitro drug release

The behavior of triclosan release from poly(4Hb-*alt*-Glc) and poly(Glc-*alt*-6HH) microspheres, illustrated in Figures 8 and 9, respectively, revealed a clear dependence on the medium's hydrophilicity. Thus, in the Sörensen medium, the amount of released drug

TABLE IV
Lamellar Sizes and Crystallinity Data of Charged and Uncharged Polyesters

Sample	T_g (°C)	T_f (°C)	ΔH_f (kJ/mol)	L_B (nm)	L_γ (nm)	l_c (nm)	X_c (%) DSC	X_c (%) WAXD	X_c (%) SAXS
Poly(4Hb-*alt*-Glc)[a]	−16	106	8.6				33	53	
Poly(4Hb-*alt*-Glc)[b]	−16	105	8.7				33		
Poly(4Hb-*alt*-Glc)[c]		105, 107	13.9	8.8	8.7	5.8	53	41	67
Poly(Glc-*alt*-6HH)[a]	−36	64	7.3				21	48	
Poly(Glc-*alt*-6HH)[b]	−34	57	6.3				19		
Poly(Glc-*alt*-6HH)[c]		45, 57	4.9, 8.5	11.5	10.1	7.4	37	45	73

ΔH_f = melting enthalpy; T_f = melting temperature; T_g = glass-transition temperature; L_B = Bragg long period; X_c = crystallinity.
[a] Sample after being quenched.
[b] Triclosan-charged sample after being quenched.
[c] Charged microsphere preparation.

quickly reached an asymptotic value that was lower than the total drug loading. It seems that the hydrophobic character of triclosan allows good interactions to be established with the polymer matrix, as also deduced from the DSC analysis and the X-ray diffraction data. Furthermore, the concentration of the released drug was always lower than the corresponding solubility limit (10–17 mg/L). It has been reported that the release of triclosan from a hydrophobic polymer matrix into an aqueous medium can be limited by the establishment of an equilibrium defined by a partition coefficient.[24] The slight difference between the percentages of triclosan released from both kinds of microspheres may reflect the higher hydrophobicity of poly(Glc-*alt*-6HH) (3% of the released drug) compared to that of poly(4Hb-*alt*-Glc) (4%).

Release profiles changed drastically when a hydrophobic cell medium was used. For both polymers, a sustained release pattern was observed for approximately 1 week. At the initial stage, a small burst effect related to the drug entrapped near the surface of the microparticles was detected. This effect was smaller for the more hydrophobic polyester derived from hydroxyhexanoic acid, which may have delayed the penetration of water into the matrix. It is well established[32,33] that the diffusion path should be filled with water to facilitate drug diffusion through amorphous regions, and consequently

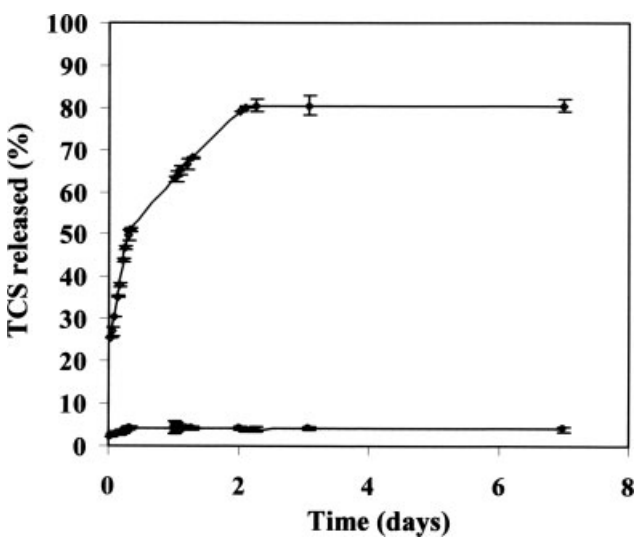

Figure 8 Experimentally measured *in vitro* drug release kinetics at 37°C and pH 7.42 for poly(4Hb-*alt*-Glc) in (◇) the cell medium and (○) the Sörensen solution. Error bars indicate the ± range for $n = 3$ (cell medium) and for $n = 6$ (Sörensen solution). TCS indicates triclosan.

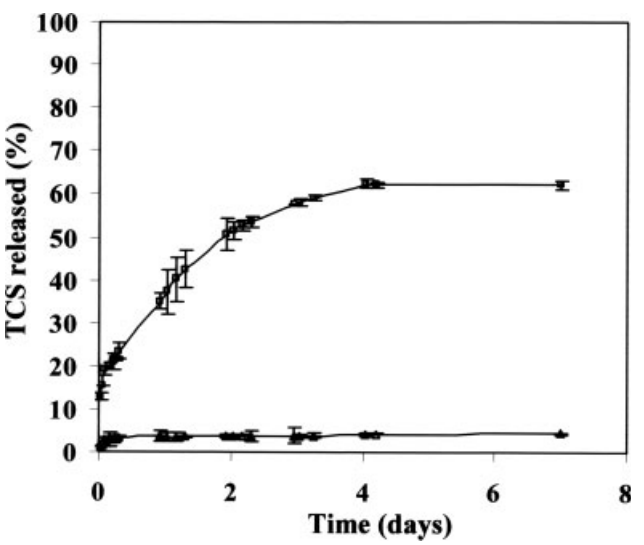

Figure 9 Experimentally measured *in vitro* drug release kinetics at 37°C and pH 7.42 for poly(Glc-*alt*-6HH) in (□) the cell medium and (△) Sörensen solution. Error bars indicate the ± range for $n = 3$ (cell medium) and for $n = 6$ (Sörensen solution). TCS indicates triclosan.

a small burst effect should be expected for a hydrophobic matrix.

It should also be pointed out that the release mechanism may be mainly controlled by channeling when a hydrophobic drug such as triclosan is used. Note that the cell medium contains high-molecular-weight solubilizing amphiphilic molecules, which can penetrate the polymer matrix through channels and pores only. In this sense, the differences in the final obtained release rates (80 and 62%) may reflect both the different morphologies and hydrophobic characters of the microspheres.

The observed release profiles can be well compared with those reported for a hydrophobic polymer matrix such as the poly(ester amide) consisting of glycine, sebacic acid, and dodecanodiol units.[34] In this case, 41 and 7% triclosan contents were released in the cell medium and Sörensen solution, respectively. These asymptotic values were obtained after 6 days in the cell medium and after 12 h in the Sörensen solution. The release of triclosan from chitosan matrices in a pH 7 phosphate-buffered solution containing a 0.5% (w/v) concentration of a surfactant was also studied for application to the oral cavity.[26] In this case, triclosan release extended over a period of 8 h, and a maximum release of 85% was attained.

The relatively high crystallinity of the samples may also have an influence on the slow release observed because lamellae can act as a barrier during drug diffusion. Bigger and more perfectly shaped crystalline lamellae should reduce the release rate and account for sustained drug release.[35,36] In fact, it has been established that the rate of drug release from polymer microspheres is significantly affected by the crystallinity of both the polymer matrix and the drug.[37,38]

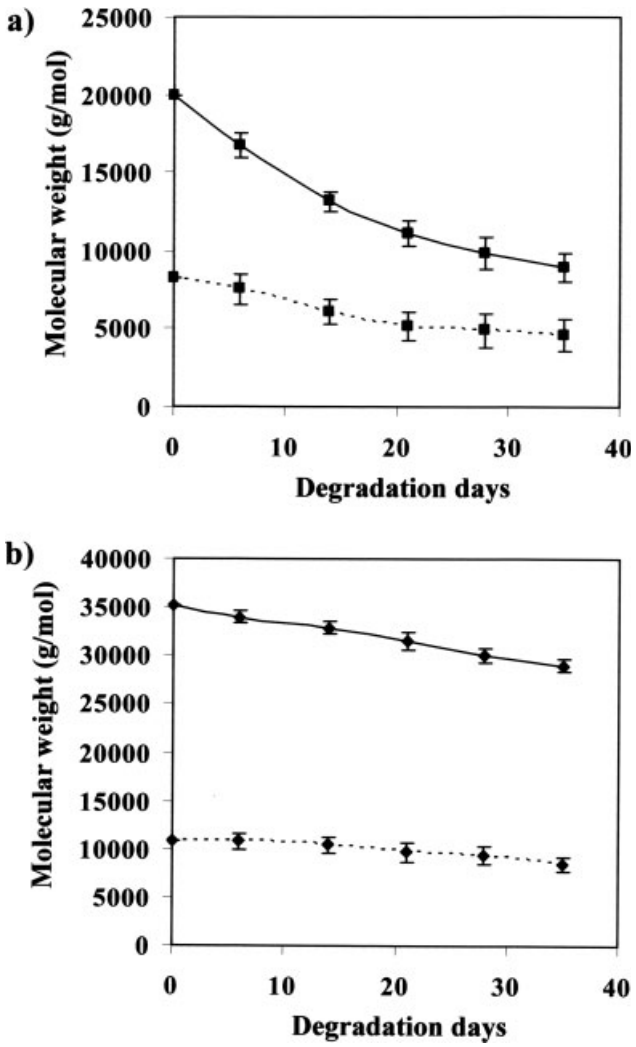

Figure 10 (- - -) Number-average and (—) weight-average molecular weights of (a) poly(4Hb-*alt*-Glc) and (b) poly(Glc-*alt*-6HH) microspheres (45–80 μm) versus the days of exposure to a pH 7.42 phosphate buffer at 37°C. Each plotted value corresponds to the average of three independent experiments.

Degradation profiles of the microspheres

Figure 10 shows the changes in the molecular weight averages for microspheres of the two studied polyesters over a period of 38 days, which was the time necessary to obtain asymptotic triclosan release. The decrease in the molecular weight was insignificant for the poly(Glc-*alt*-6HH) sample, although the weight-average value was slightly sensitive to water exposure. This feature suggests that the hydrolysis of ester groups was higher for the longer molecules, presumably because of their larger ester content. The weight of the microspheres remained practically constant during exposure to the hydrolytic medium, a weight loss of only 2% being determined after 38 days. The indicated data clearly demonstrate that triclosan release cannot be associated with a release controlled by polymer erosion. Poly(4Hb-*alt*-Glc) samples were more sensitive to degradation, probably as a result of their higher hydrophilicity and lower initial molecular weight. In this case, the change in the weight-average molecular weight was more significant, but the weight loss (4% after 38 days of exposure) was sufficiently low to rule out significant polymer erosion. Two other mechanisms for controlling drug release from biodegradable polymers[39] have been identified, that is, Fickian diffusion through the polymer matrix and diffusion through matrix pores. These mechanisms appear to be the relevant ones for the release of the studied microspheres.

Release kinetics in cell media

The behavior of triclosan release from the new polyester microspheres in the aforementioned cell medium can be well described by the Baker–Londsdale

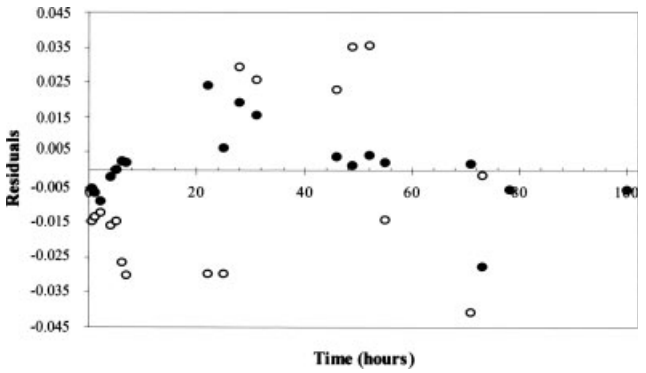

Figure 11 Plot of residuals for triclosan release from (○) poly(4Hb-*alt*-Glc) and (●) poly(Glc-*alt*-6HH) microspheres fitted to the Baker and Lonsdale model.

model,[40] which was formulated for drug release from diffusion-rate-limiting matrices of a spherical shape obeying the following equation:

$$\frac{3}{2}\left[1-(1-M_t/M_\infty)^{2/3}\right]-M_t/M_\infty = kt \qquad (1)$$

where M_t is the mass released at time t, M_∞ is the mass released at the asymptotic saturation level, and k is the release kinetic constant. For the calculation of the equation, only the drug release after an initial period of 30 min was considered to avoid complications due to non-steady-state behavior, which usually appears within the first minutes of the experiment.

The regression analysis was performed for the entire profile [from 0.5 to 48 h (hydroxybutyric derivative) and from 0.5 to 100 h (hydroxyhexanoic derivative)]. A kinetic constant of 0.0085 h^{-1} was found for poly(4Hb-*alt*-Glc), whereas a lower value of 0.0044 h^{-1} was determined for the hydroxyhexanoic derivative. In this case, a very good correlation was observed ($R = 0.996$), indicating that the chosen model was perfectly appropriate to describe triclosan release. Slightly worse agreement was found for poly(4Hb-*alt*-Glc) ($R = 0.986$), although the model can still be considered adequate. The times required for 50% drug release, determined from the deduced kinetic constants, were clearly different. Thus, this series of materials based on the change of the ω-hydroxyl acid unit may be interesting for obtaining a tailored release. The half-time values of 6.6 and 12.5 h for the hydroxybutyric and hydroxyhexanoic derivatives, respectively, were a result of the large difference in the diffusion rate between the microspheres of the two studied polymers.

A graphical analysis of the residuals was performed to gain insight into the quality of the fitting, as shown in Figure 11 for the two studied copolyesters. The residuals appeared to be randomly scattered around zero, and this suggested that the experimental data did not depart from the theoretical values significantly. The absolute values of the residuals were higher for the poly(4Hb-*alt*-Glc) microspheres, and this was in agreement with a worse correlation coefficient.

Drug release controlled by diffusion from spherical particles can be described according to Fick's second law of diffusion,[41] which can lead to a simplified solution when the diffusional resistance within the polymeric matrices is predominant.[42] Thus, the apparent diffusion coefficient of the drug (D) can be evaluated as follows:

$$\frac{M_\infty - M_t}{M_\infty} = \frac{6}{\pi^2}\sum_{n=1}^{\infty}\frac{1}{n^2}\exp\left(-\frac{n^2\pi^2}{R^2}Dt\right) \qquad (2)$$

where R is the radius of the microsphere.

The goodness of fit between the experimental and theoretical $(M_\infty - M_t)/M_\infty$ values was determined from both the calculated mean squared deviation and the root mean squared scaled deviation, which scale each deviation by the standard error of the mean of the data. For both polymer matrices, the fit was not significantly improved when more than three terms were considered in the summatory function of eq. (2). In agreement with the previous analysis, a lower diffusion coefficient and a better fit model were deduced for the hydroxyhexanoic acid derivative. Thus, on the basis of an average radius of 30 μm, the diffusion coefficients were 6.1×10^{-12} and 1.5×10^{-11} cm^2/s, whereas the mean squared deviation values were 0.0012 and 0.0019, for poly(Glc-*alt*-6HH) and poly(4HB-*alt*-Glc) samples, respectively. Figure 12 shows a good agreement between the experimental release data of both polymers and the corresponding release curves calculated under the assumption of eq. (2) and the aforementioned diffusion coefficients.

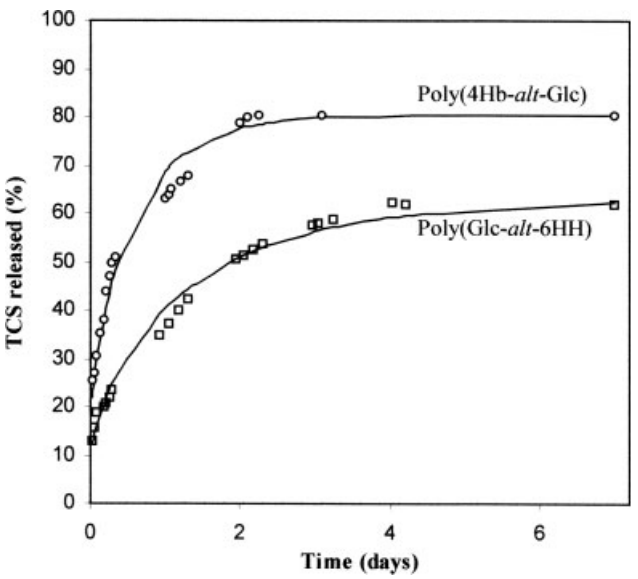

Figure 12 Theoretically calculated (solid lines) and experimental (symbols) triclosan release from poly(4Hb-*alt*-Glc) and poly(Glc-*alt*-6HH) matrices. TCS indicates triclosan.

CONCLUSIONS

Two new copolyesters consisting of glycolic acid and hydroxybutyric or hydroxyhexanoic acid units have proved to be adequate for preparing microspheres with sustained release of hydrophobic drugs such as triclosan. Release in a hydrophobic cell medium is well described by the Baker–Londsdale model, which is based on a diffusion process in spherical particles. Degradation data allow release controlled by polymer erosion to be ruled out, although channeling may be significant in microparticles prepared from poly(4Hb-*alt*-Glc) because of their high porosity and rough surface. The different release behaviors of the two studied polymers may reflect differences in porosity and hydrophobicity because both factors enhance release from the hydroxybutyric acid derivative. Triclosan has a good affinity to the two studied polymer matrices and seems to be present in both the amorphous and crystalline phases. The prepared charged microspheres had high crystallinity and a microstructure defined by the presence of lamellar stacks and amorphous domains. Finally, the two copolyesters have very different thermal properties (e.g., melting and glass-transition temperatures), and this is interesting because it may influence chain mobility in amorphous phases and consequently the drug diffusion rate. However, the release data suggest that interactions between the polymer matrix and the drug are the main factors affecting the diffusion coefficient because it increases for the less hydrophobic sample, although it has the greatest glass-transition temperature. It is worth noting that any change in the nature of the glycolic acid comonomer has a significant impact on the properties, which may be interesting for general applications.

The authors are thankful to Montse Marsal of the Department of Materials for the scanning electron micrographs. They express their gratitude to François Fauth and Ana Labrador of the CRG BM16 beam line staff of the Consortium for the Exploitation of the Synchrotron Light Laboratory.

References

1. Langer, R. Nature 1998, 392, 5.
2. Uhrich, K. E.; Cannizaro, S. M.; Langer, R. S.; Shakesheff, K. M. Chem Rev 1999, 99, 3181.
3. Kumar, M. N. V. R.; Kumar, N.; Domb, A. J.; Arora, M. Adv Polym Sci 2002, 160, 45.
4. Vert, M.; Li, S. M.; Spenlehauer, G.; Guerin, P. J Mater Sci: Mater Med 1992, 3, 432.
5. Edlund, E.; Albertssson, A. C. J Polym Sci Part A: Polym Chem 1999, 37, 1877.
6. Kulkarni, R. K.; Moore, E. G.; Hegyeli, A. F.; Leonard, F. J Biomed Mater Res 1971, 5, 169.
7. Kricheldorf, H. R.; Kreiser-Saunders, I.; Jürgens, C.; Wolter, D. Macromol Symp 1996, 103, 85.
8. Thombre, A. G.; Cardinal, J. R. Encyclopedia of Pharmaceutical Technology; Marcel Dekker: New York, 1990; Vol. 2, p 61.
9. Mädder, K.; Gallez, B.; Liu, K. J.; Swartz, H. M. Biomaterials 1996, 17, 457.
10. Zhu, G. Z.; Mallery, S. R.; Schewendeman, S. P. Nat Biotechnol 2000, 18, 52.
11. Benita, S. Microencapsulation: Methods and Industrial Applications; Marcel Dekker: New York, 1996.
12. Martínez-Palau, M.; Franco, L.; Ramis, X.; Puiggalí, J. Macromol Chem Phys 2006, 207, 90.
13. Martínez-Palau, M.; Franco, L.; Puiggalí, J. Macromol Chem Phys 2008, 209, 393.
14. Epple, M.; Kirschnick, H. Chem Ber 1996, 129, 1123.
15. Schwarz, K.; Epple, M. Macromol Chem Phys 1999, 200, 2221.
16. Epple, M.; Kirschnick, H. Liebigs Ann 1997, 81.
17. Herzberg, O.; Epple, M. Eur J Inorg Chem 2001, 1395.
18. Katz, A. R.; Mukherjee, D. P.; Kagonov, A. L.; Gordon, S. A. Sur Gyn Obst 1985, 161, 213.
19. Bezwada, R. S.; Jamiolkowski, D. D.; Lee, I. Y.; Agarwal, V.; Persivale, J.; Trenka-Bethin, S.; Erneta, M.; Suryaderwara, J.; Yang, A.; Liu, S. Biomaterials 1995, 16, 1141.
20. Chu, C. C.; Zhang, L.; Coyne, L. D. J Appl Polym Sci 1995, 56, 1275.
21. Martínez-Palau, M.; del Valle, L.; Gámez, A.; Sepulcre, F.; Puiggalí, J. J Appl Polym Sci.
22. Bhargava, H. N.; Leonard, P. A. Am J Infect Control 1996, 24, 209.
23. Rothenburger, S.; Spangler, D.; Bhende, S.; Burkley, D. Surg Inf 2002, 3, S79.
24. Zurita, R.; Puiggalí, J.; Rodríguez-Galán, A. Macromol Biosci 2006, 6, 58.
25. Kockish, S.; Rees, G. D.; Young, S. A.; Tsiboukis, J.; Smart, J. D. J Pharm Sci 2003, 9, 1614.
26. Kockish, S.; Rees, G. D.; Young, S. A.; Tsiboukis, J.; Smart, J. D. Eur J Pharm Biopharm 2005, 59, 207.
27. Maestrelli, F.; Mura, P.; Alonso, M. J. J Microencapsul 2004, 21, 857.
28. CORFUNC. http://www.ccp13.ac.uk/software/program/corfunc/corfunc.htm (accessed May 2008).
29. de Rosa, G.; Quaglia, F.; la Rotonda, M. I.; Appel, M.; Alphandary, H.; Fatal, E. J Pharm Sci 2002, 91, 790.
30. Yang, Q.; Owusu-Ababio, G. Drug Dev Ind Pharm 2000, 26, 61.
31. Davids, D. J.; Misra, A. Relating Materials Properties to Structure; Technomic: Lancaster, PA, 1999.
32. Langer, R.; Folkman, F. Nature 1976, 263, 797.
33. Langer, R. Science 1990, 249, 1527.
34. Vera, M.; Puiggalí, J.; Coudane, J. J Microencapsul 2006, 23, 686.
35. Miyajima, M.; Koshika, A.; Okada, J.; Kusai, A.; Ikeda, M. J Controlled Release 1998, 56, 85.
36. Miyajima, M.; Koshika, A.; Okada, J.; Ikeda, M. J Controlled Release 1999, 61, 295.
37. Izumikawa, S.; Yoshioka, S.; Aso, Y.; Takeda, Y. J Controlled Release 1991, 15, 133.
38. Mijayima, M.; Koshika, A.; Okada, J.; Ikeda, M.; Nishimura, K. J Controlled Release 1997, 49, 207.
39. Jalil, R.; Nixon, J. R. J Microencapsul 1990, 7, 297.
40. Baker, R. W.; Londsdale, H. K. Controlled Release of Biologically Active Agents; Plenum: New York, 1974; p 15.
41. Crank, J. The Mathematics of Diffusion; Clarendon: Oxford, 1975.
42. Siepmann, J.; Elkharraz, K.; Siepmann, F.; Klose, D. Biomacromolecules 2005, 6, 2312.